frontiers | Frontiers in Marine Science

TYPE Original Research
PUBLISHED 31 March 2025
DOI 10.3389/fmars.2025.1555911

OPEN ACCESS

EDITED BY
Luca Rindi,
University of Pisa, Italy

REVIEWED BY
Laura Ghigliotti,
National Research Council (CNR), Italy
Americo Montiel,
Universidad de Magallanes, Chile

*CORRESPONDENCE
Bodil A. Bluhm
bodil.bluhm@uit.no

RECEIVED 05 January 2025
ACCEPTED 10 March 2025
PUBLISHED 31 March 2025

CITATION
Dinevik H, Altenburger A and Bluhm BA (2025) Slow growth and high longevity characterize the common, large Arctic brittle star, *Ophiopleura borealis*. *Front. Mar. Sci.* 12:1555911. doi: 10.3389/fmars.2025.1555911

Slow growth and high longevity characterize the common, large Arctic brittle star, *Ophiopleura borealis*

Hanna Dinevik[1,2,3], Andreas Altenburger[2] and Bodil A. Bluhm[1*]

[1]Department of Arctic and Marine Biology, UiT The Arctic University of Norway, Tromsø, Norway,
[2]The Arctic University Museum of Norway, UiT The Arctic University of Norway, Tromsø, Norway,
[3]Department of Biology Education, Stockholm University, Stockholm, Sweden

The longevity (lifespan) and growth rates of a given species provide the basis for estimating its contributions to secondary production and energy flow in an ecosystem, for guiding management decisions, and determining recovery times after disturbances. For brittle stars, a class of echinoderms that dominate the megabenthos in various marine systems due to their often large populations, including those on Arctic soft bottom shelves, growth and longevity information can be estimated through growth bands in their ossicles (arm bones). Here, we estimated the maximum life span, age distribution, and growth rate of the common, large Arctic endemic brittle star, *Ophiopleura borealis*, from the northern Barents Sea. We counted growth bands in trawl-caught specimens using scanning electron microscope images of the innermost arm ossicles of 80 specimens spanning the known size range. These counts were corrected for overgrowth of the earliest growth bands, and growth parameters were estimated using common growth models. The age bands appeared as alternating layers of dense and less dense lines in the stereom of the ossicle fossae. The maximum corrected age band count was 39, which we infer as reflecting the age in years. This estimate is higher than for most other studied brittle stars, including polar species. Most individuals in the sampled population spanned estimated ages from 25-32 years. The growth constant k estimates of 0.09 from the Single logistic growth model and 0.01 from the specialized van Bertalanffy model indicate slow growth. The combined slow growth rate and long lifespan in Arctic brittle stars suggest that the large stocks found in Arctic regions may take a substantial time period to establish and recover from potential disturbances.

KEYWORDS

Arctic, benthos, brittle star, growth, longevity, Ophiuroidea, *Ophiopleura borealis*

1 Introduction

Longevity and growth rates are key traits in the population dynamics of any living organisms and are typically related to each other. Generally, fast-growing species tend to have shorter life spans compared to slow-growing species (Dantzer and Fletcher, 2015; Salguero-Gómez and Jones, 2017). These traits are also linked to the age at which a species reaches maturity and to their contribution to secondary production, carbon storage, and cycling. Consequently, they provide important knowledge in both species management as well as in energy flow models in food webs (Pedersen et al., 2008; Moore and de Ruiter, 2012) and carbon budgets (Stearns and Koella, 1986). Slow growth rates and high longevity, often spanning decades, are typical for marine invertebrates in high-latitude, cold-water environments, and areas with limited food availability, such as polar regions and the global deep-sea (Bluhm et al., 1998; Pörtner et al., 2005; Neves et al., 2015; Peck, 2016; Ravelo et al., 2017). Depauperate food conditions can limit growth either seasonally or permanently (Levin et al., 2010). The longevity and growth rates of a species can be linked to its vulnerability; slow-growing marine benthic invertebrates often require years or even decades to recover from disturbances in cold water (Beuchel and Gulliksen, 2008; Al-Habahbeh et al., 2020). Differences in recovery rates from disturbances have been observed across different latitudes (Al-Habahbeh et al., 2020), suggesting increased vulnerability in polar and deep-sea organisms (Bonfim et al., 2024).

Age and growth data are missing for many common cold-water species either because these species lack hard structures that could record age bands or because tracking a population through an entire lifespan of decades is unrealistic. For echinoderms, however, a phylum in which members can dominate megabenthos stocks in both hard-bottom and soft-bottom systems (Lebrato et al., 2010; Jørgensen et al., 2015), growth bands validated to reflect chronological age form in their calcareous structures, such as test plates or arm bones, allowing for estimates of longevity and growth rates. Among echinoderms, brittle stars (Ophiuroidea) constitute the most species-rich living class, with more than 2000 extant species described (Stöhr et al., 2012). Brittle stars fulfil multiple ecological roles: Despite their high carbonate content and low caloric value, brittle stars are preyed upon by some crab and fish species (Hinz et al., 2005; Hüssy et al., 2016; Burukovsky et al., 2022). They may form dense aggregations at the seafloor (Fujita and Ohta, 1989; Broom, 2009; Calero et al., 2018) of 100s to more than 7000 individuals m^{-2} and at such densities enhance biogeochemical fluxes and oxygen supply through bioturbation (Davoult and Migné, 2001: Wood et al., 2008; Davoult et al., 2009) contributing substantially to carbon remineralization (Vopel et al., 2003; Broach et al., 2016; Murat et al., 2016). Suspension feeding brittle star species may also support benthic-pelagic coupling (Ambrose et al., 2001; Blicher and Sejr, 2011).

In terms of both biomass and abundance, in the cold waters of Arctic shelves, brittle stars are one of the dominating groups in epibenthic communities (Piepenburg and Schmid, 1996; Piepenburg et al., 1997; Bluhm et al., 2009; Ravelo et al., 2014, 2017). They may contribute more than 50% of the wet weight biomass and abundance to total epibenthos stocks (Piepenburg, 2000; Ravelo et al., 2014). Peak abundances of approximately 500 brittle star individuals per m^2 were reported in the Barents Sea and Laptev Sea (Piepenburg and Schmid, 1996; 1997), though densities of 30-400 individuals per m^2 appear to be more common (Fujita and Ohta, 1990; Piepenburg, 2000). Among the circa three dozen brittle star species occurring in Arctic seas, *Ophiopleura borealis* (Danielssen and Koren, 1877) (Figure 1A) is endemic to the region. It is commonly found throughout most of the area (Piepenburg and Schmid, 1996; Smirnov et al., 2014; Udalov et al., 2018; Zhulay et al., 2019; Yunda-Guarin et al., 2022) at depths from 40 to 1400 m (Piepenburg, 2000). *O. borealis* is a common species in the Barents and Kara Seas (Galkin et al., 2010a, 2010, 2015; Jørgensen et al., 2015; Pavlova et al., 2023). Relatively little is known about the life history and biology of *O. borealis*, other than that it is a large-bodied (maximum disc diameter greater than 4 cm) scavenger and deposit feeder with a pelagic ophiopluteus larva and small eggs (Piepenburg and Von Juterzenka, 1994; Gallagher et al., 1998). While data on growth and longevity of other common Arctic brittle star species

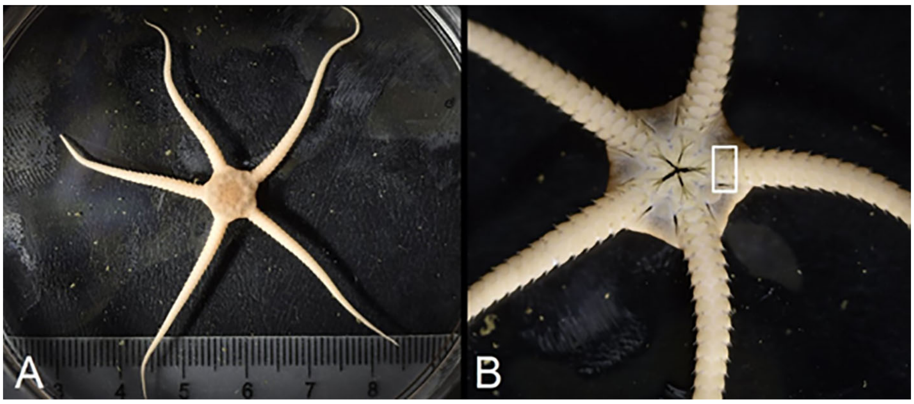

FIGURE 1
Aboral **(A)** and oral **(B)** view of a live specimen of the Arctic endemic brittle star *Ophiopleura borealis*. The white rectangle in **(B)** marks the part of the arm containing the innermost ossicle used in band count analysis. Reproduced with permission from Fredrik Broms, https://www.northernlightsphotography.no/.

have recently been generated (Ravelo et al., 2017; Stratanenko and Denisenko, 2020; Stratanenko, 2021), no such data are available for *O. borealis* yet but would help anticipate the effects of disturbances on the species and the Arctic benthic ecosystem at large.

The goal of this study was, therefore, to provide estimates of age and growth parameters of *O. borealis* specimens. The study area, the northern Barents Sea in the Atlantic Arctic gateway, is a cold-water shelf sea characterized by high seasonality in light (including a period of polar night), primary production, vertical carbon flux, and ice cover (Jakobsen and Ozhigin, 2011). It is also increasingly exposed to perturbations from bottom trawling (Jørgensen et al., 2016), risks related to petroleum production (Aven and Renn, 2012), and climate warming, which drives changes such as species distribution shifts (Calvet et al., 2024) and alterations in the food web (Kortsch et al., 2012). We expected, first, that growth bands would be present in *O. borealis* due to the seasonally variable habitat. Second, we hypothesized that *O. borealis* would have slow growth (as indicated by a low growth constant estimated from common growth models) and high longevity (on the order of decades). We compared growth metrics and longevity to brittle stars from lower latitudes.

2 Materials and methods

2.1 Sample collection

Specimens of *Ophiopleura borealis* (Figure 1) were collected from the northern Barents Sea in November 2017 onboard R/V Helmer Hanssen as part of the Arctic PRIZE project (Hopkins, 2018) at a depth of 167 m at 77.46183°N and 27.629693°E (station B4). A 2-m beam trawl with a mesh size of 25 mm and 4 mm in the cod-end was towed at a speed of 1.5 knots for 3 minutes on the seafloor. Additional specimens were collected in August 2018 onboard R/V Kronprins Haakon as part of the Nansen Legacy Project at a depth of 284 m at 78.8231°N and 34.2506°E (station P3/NLEG07) (Ingvaldsen et al., 2020). Here, a Campelen 1800 trawl with an 8 mm mesh size in the cod-end was towed for 15 minutes on the seafloor at 3 knots. In both cases, the catch was sorted by taxa, and specimens of *O. borealis* were then frozen in plastic bags at -20 °C. Bottom temperatures in the area were 3 °C (2017) and 1 °C (2018) at the time of sampling, which is representative for the area (Skagseth et al., 2020). A total of 142 specimens of *O. borealis* was selected from the Barents Sea samples.

Due to a lack of very small specimens from the Barents Sea collection, small *O. borealis* were supplemented from the Northeast Greenland shelf during a cruise on the R/V Kronprins Haakon as part of the TUNU programme (Christiansen, 2012) in August 2022. The same Campelen 1800 trawl used in the Barents Sea was deployed at a depth of 447 m at 75.977°N and 20.313°W (station Besselfjord) and towed for 10 minutes at the bottom at 3 knots. While this supplementation is not ideal, the latitude was close to that from station B4 in the Barents Sea, and the bottom temperature in the area was similar at -1.5 to 1.6 °C. A total of 36 individuals was added to the Barents Sea specimens from Northeast Greenland.

2.2 Body size measurements

The frozen specimens were thawed in a sealed container in a 60° C-water bath for 10-20 minutes, depending on the size of the specimens. Once thawed, the specimens were blotted dry and photographed, aboral side up, using a Sony A7 III digital camera with a size scale included for subsequent size measurements from the digital images. For each specimen, the disc diameter (DD) was measured up to three times in ImageJ (Schneider et al., 2012) from the base of one arm to the opposite disc edge, to obtain a mean DD accurate to the nearest tenth of a mm. Individuals were assigned to 0.5 cm-interval DD bins, and a minimum number of N=10 was chosen from each bin for subsequent age band readings, with the exception of the smallest and largest size bins where fewer specimens were available.

2.3 Preparation of arm ossicles

Each arm was dissected to extract the arm bones (ossicles) closest to the jaws (Figure 1B). These are the oldest ossicles (Stöhr et al., 2012) and, hence, contain age bands covering the entire lifespan. Any remaining tissue on the ossicles was removed by submerging them in vials with 4-16% sodium chlorite, which were warmed to 60°C in a water bath for 10-20 min following Ravelo et al. (2017). Ossicles less than approximately 1.5 mm wide from the smallest individuals were subjected to room temperature. The ossicles were then washed in MilliQ water and subsequently in 70% ethanol (Dahm, 1993; Orino et al., 2019). The cleaned and dried ossicles were mounted on aluminum pin stubs (12.7 mm diameter, Micro to Nano) using conductive carbon tape, and sputter-coated with gold for two 15-second cycles in a JEOL JFC-1300 auto fine coater on their proximal or distal surface. This amount of coating was found to yield clearly visible growth bands in the JEOL NeoScope JCM-7000 Scanning Electron Microscope (SEM), while additional coating tended to clog the stereom pores.

Ossicles from a total of 85 individuals were photographed in the SEM, selecting those with at least three intact ossicles available. Ossicles from a few additional individuals in each size group were also photographed when available, in case images from any ossicles proved unsuitable for image analysis. Images were deemed unsuitable if damage to the ossicle, remaining tissue, or low focus made the ossicle growth bands unreadable. Ossicle diameter (OD) was measured directly in the SEM as the widest horizontal distance between the fossae edges, excluding ossicles missing large parts of fossae due to damage. A linear regression model was applied to the mean OD and DD of individuals, to check if size increased proportionally.

2.4 Age band count and correction

SEM images of ossicles from 80 individual brittle stars were analyzed in ImageJ (Schneider et al., 2012). The remaining five individuals in the photographed sample were excluded from the analyses due to low visibility of growth bands. The aim was to analyze three ossicles per individual, but in some cases, lost or damaged ossicles resulted in fewer ossicles analyzed. Generally, the smaller an individual was, the more fragile the ossicles were.

Growth band analysis was done on the upper left and right fossa of the ossicles by marking and numbering each band in ImageJ (Figure 2, marks shown in the left fossa). A growth band was defined as the combination of two adjacent streaks of differing stereom densities, typically visible as alternating dark and light streaks on the fossa surface (Ravelo et al., 2017), sometimes with associated ridges (Gage, 1990a; Dahm, 1993; Gage, 2003). The density changes were validated to reflect annual growth patterns in studies of other brittle stars and sea urchins from areas with distinct seasonal variations (Gage, 1992; Brey et al., 1995; Sun et al., 2019); hence we equal one pair of light and dark growth bands to one year of growth also in the present study.

A correction is needed when translating band counts to age because the articulating middle part of ossicles expands as an individual grows, obscuring the inner bands on the fossae (Dahm and Brey, 1998). To correct for growth bands covered by this overgrowth, a procedure similar to that used by Ravelo et al. (2017) and Dahm and Brey (1998) was applied (see Supplementary Material for a description). The estimated number of hidden bands in each individual was then added to the initial count of visible bands. The final sum was assumed to correspond to the number of years and is referred to as the corrected age of a given individual.

2.5 Data analysis

Data analysis was conducted using the statistical software R (R Core Team, 2023), with R packages including ggpmisc (Aphalo, 2016), ggplot2 (Wickham et al., 2007), ggpubr (Kassambara, 2023), minpack.lm (Elzhov et al., 2022), and dplyr (Wickham et al., 2014).

The specialized von Bertalanffy (Equation 1) and Single logistic (Equation 2) growth functions were applied to the size-at-corrected-age data, with the goal of estimating the growth constant *k* and asymptotic size S_∞ (from both models), as well as the age at the inflection point t* (from the Single logistic model). We used these two models, because the former model is the most commonly used one in the invertebrate literature therefore allowing many comparisons; given it yielded an unrealistic S_∞, however, we also included the latter model, which in addition estimates the point above which growth rate declines (Brey, 2001).

$$S_t = S_\infty \times (1 - e^{-k \times (t - t_0)}) \quad (1)$$

$$S_t = S_\infty \div (1 + e^{-K(t - t^*)}) \quad (2)$$

To initiate the model runs, starting values for *k* and t_0 and (the age in which size is 0) were required and obtained by calculating a linear regression of size on corrected age data. The slope was used as a starting value for parameter *k*, while the intercept on the y-axis was used for t_0. The output from each growth model was used to plot the corresponding growth curve, and the Akaike Information Criterion for small sample size along with *RSS* and R^2 values were calculated to compare the goodness-of-fit using the R package AICcmodavg (Mazerolle, 2023). The growth performance index φ′ (Equation 3) was calculated for *O. borealis* and, when possible, for brittle star species from other climatic zones, as described by Brey (2001). This calculation used the asymptotic size and growth constants estimated by either the specialized or generalized von Bertalanffy growth function, depending on what the publications provided.

$$\phi' = \log(\mathrm{K}) + 2\log(S_\infty) \quad (3)$$

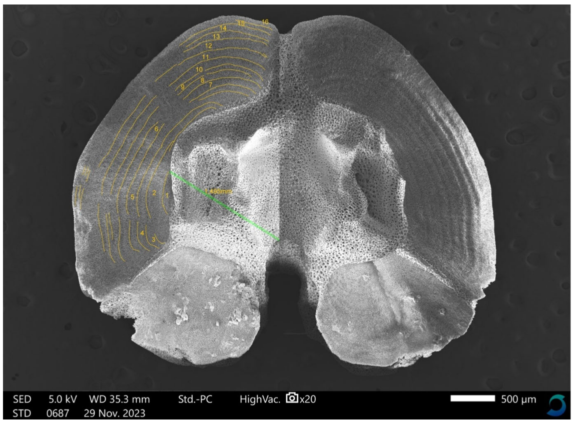

FIGURE 2
Scanning electron micrograph image of an ossicle of *Ophiura borealis* from the Barents Sea. On the left ossicle fossa age bands are marked and numbered in yellow, and MP-VB1 distance is marked (green). From Reigstad et al., in press, under a CC BY 4.0 license.

3 Results

3.1 Size distribution

In the 177 individuals from the combined Barents Sea and NE Greenland shelf samples, DD ranged from 0.75-4.26 cm, with an overall mean of 2.50 cm (Figure 3A). One individual was excluded from the DD measurements due to the disc being broken. The distribution of DD measurements in the full dataset appeared bimodal with the size mode (DD > ca. 2.00 cm) constituting the majority of the individuals. Both very large and very small individuals (DD ≥ 4 cm and DD ≤ 1.00 cm, respectively) were sparse in the sample. In the subset of 80 individuals used for age analysis, a similar size distribution was chosen (Figure 3B).

Mean ODs of individuals ranged from 1.22 to 5.75 mm. DD and OD were linearly related ($y = -0.171 + 0.68x$, $R^2 = 0.95$, $p<0.05$) (Figure 4).

3.2 Presence and appearance of bands in ossicles

The alternating dark and light streaks created a pattern of growth bands in the fossae of the innermost arm ossicles of

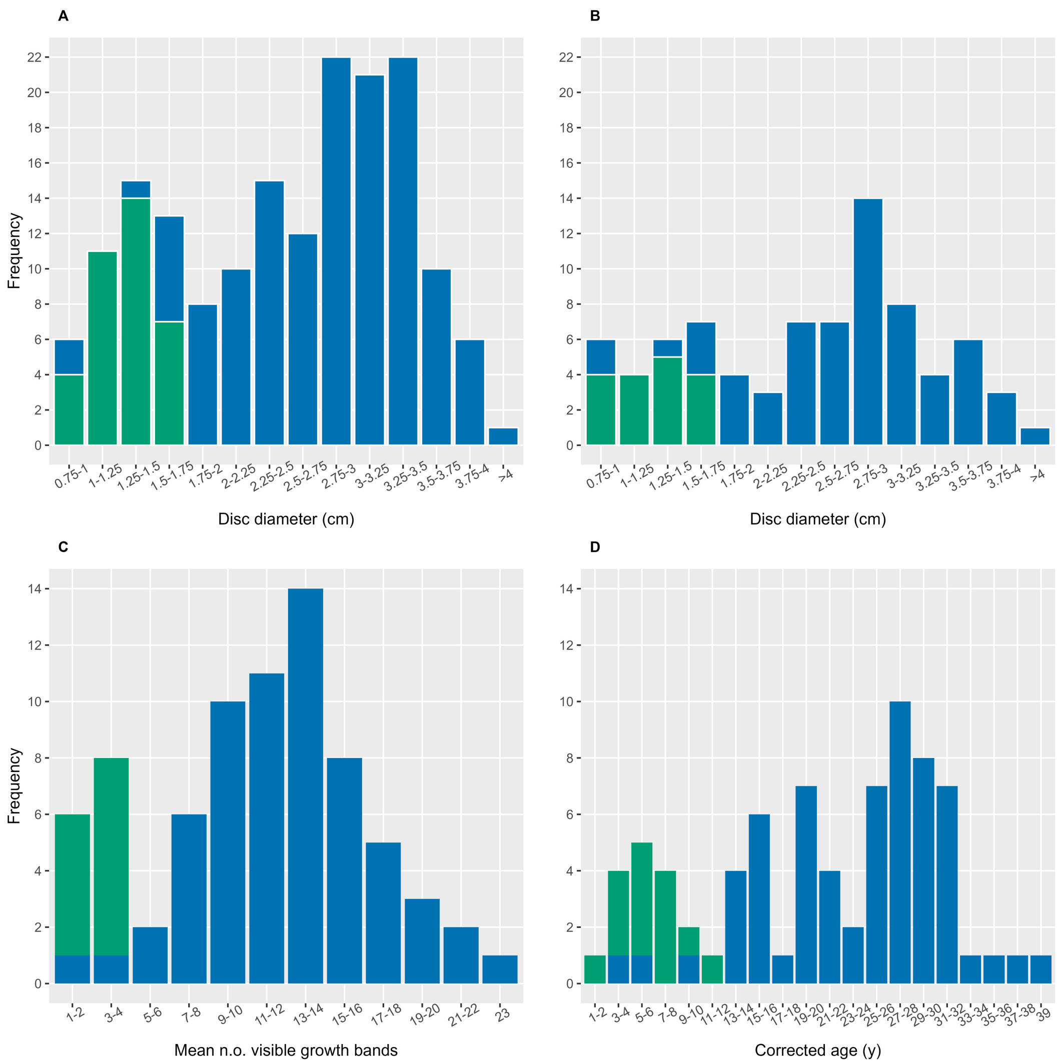

FIGURE 3
Histograms showing the distribution of disc diameter, ossicle band counts and age of *Ophiopleura borealis* from the Barents Sea. Small individuals were supplemented from the NE Greenland shelf. **(A)** Mean disc diameter of all individuals (n=177) of *O. borealis* measured, and **(B)** of individuals used in age analysis (n=80). **(C)** Distribution of mean number of visible growth bands per individual (n=80), and **(D)** estimated the age distribution following age correction (n=80). Blue: Barents Sea individuals, green: Greenland shelf individuals. For age correction see Supplementary Table S1.

O. borealis. These bands were caused by changes in stereom density and elevated ridges on the fossa surface (Figure 2). Growth bands were observed in all the examined ossicles, regardless of which side was photographed, except for a few ossicles that exhibited abnormal looking stereom growth. While growth band width was not measured, it was evident that it varied within a given ossicle, with generally narrower bands in the outermost layers (representing the most recent years of growth) in larger individuals. Areas with denser stereom typically appeared brighter in SEM images compared to less dense areas, while ridges appeared brighter on the side facing the electron beam. Areas featuring ridges and density changes often coincided.

In some instances, the articulation on the proximal side of the ossicles was damaged in such a way that the fossa surface became visible underneath. This revealed, at times faintly discernable, growth bands that were otherwise hidden, again confirming the need for band correction.

3.3 Age band counts and growth model

The established baseline for overgrown growth bands allowed for corrections of between 1-20 hidden bands, within a distance of 0.59-2.28 mm from ossicle mid-point (MP) to first visible band (VB1). The full baseline is presented in Supplementary Table S1.

The number of visible growth bands (without correction) in the n=80 individuals ranged from 1 to 23 (Figure 3C), with a mean band count of 11. Almost 20% of the individuals had 1-4 bands,

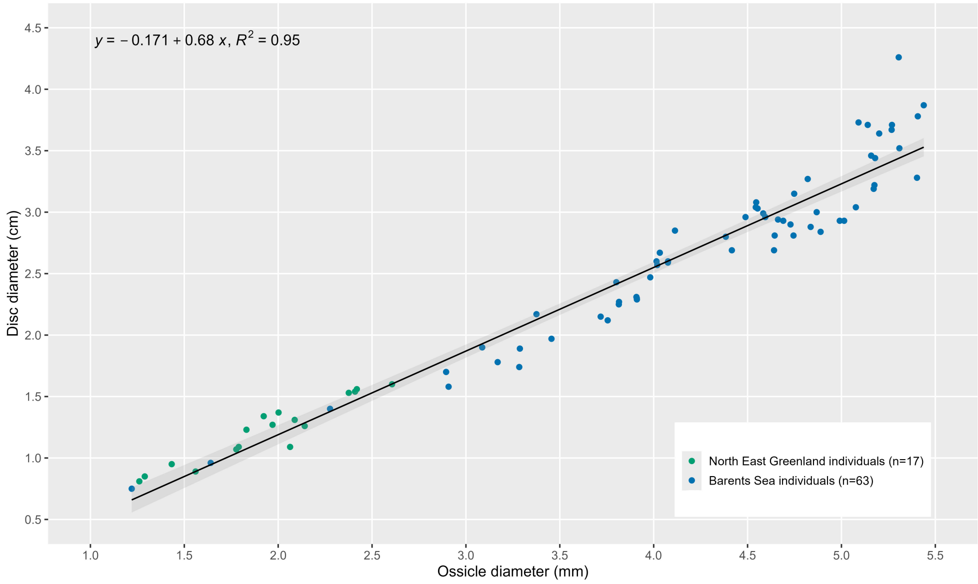

FIGURE 4
Relationship of ossicle diameter and disc diameter. Linear regression equation is given with R^2-value and 95% confidence intervals (gray shade) are shown.

while half of the individuals analyzed contained 9-16 bands. After applying the age band correction, the mean number of bands in brittle stars ranged from 1 to 39, with band counts inferred to represent years of age (Figure 3D). There was some variability in age band readings from ossicles of the same individual (Figure 5A, Supplementary Table S2). After band count correction, the mean corrected age was 21 years. In the histogram of corrected ages, similar fractions of individuals (~10-15% each) were represented in modes at age estimates of 3–8 years, 13-16 years, and 17-20 years, while 40% of all individuals were aggregated in a mode estimated at 25-32 years.

The growth constant k was estimated to be less than 0.1 by both models, although the estimates differed between growth models (Table 1). The Single Logistic model estimated the asymptotic size S_∞ to be close to the maximum size observed in our sample, while the von Bertalanffy model provided no reasonable estimate. The age at the inflection point t^* was estimated to be around 16 years by the Single Logistic model. The AICc value for the Single Logistic model was lower than for the van Bertalanffy model (Table 1). Both functions showed a high R^2 value of 0.90 with slightly lower *RSS values* for the Single Logistic model than for the von Bertalanffy model fit. Larger individuals were generally estimated to be older (Figure 5B). However, size-at-age and age-at-size were more variable in larger, older specimens, especially those >3 cm in DD and 25 years of age, respectively, than in smaller and younger individuals.

Growth performance (φ′) was estimated at 2.07 for *O. borealis.* For 20 out of the 25 brittle star species for which growth data were compiled from various climatic zones, specialized or generalized von Bertalanffy parameters were available for calculating growth performances which ranged from -0.55 to 4.99 (Table 2). The lowest k values were estimated for high latitudes, yet the relationship of k with latitude (Figure 6A) was not significant (p=0.087), and neither was the one of φ′ with latitude (Figure 6B; p=0.195). Variability in both k and φ′ was substantial.

4 Discussion

4.1 Ossicle bands

Growth bands were present in the ossicles of *Ophiopleura borealis* from both the Barents Sea and smaller individuals from the Northeast Greenland shelf. Their appearance was consistent with growth bands described in other brittle stars (Dahm, 1993: Baltic Sea; Dahm and Brey, 1998: Antarctic; Gage, 1990a; Gage, 1990b: NE Atlantic; Ravelo et al., 2017: Beaufort Sea; Stratanenko and Denisenko, 2020: Pechora Sea). By reading age bands in up to three ossicles per individual – a time-consuming task otherwise rarely done - we establish that the readability of the age bands varies somewhat within a given individual, affecting the age estimates. This variability in readability was partly caused by partial clogging of pores from gold-coating, variations in image quality, and in some cases, atypical ossicle morphology. We, therefore, suspect that earlier studies may also have introduced methodological uncertainties, leading to some bias in age bands that was not inherent to the actual band variation among individuals.

While we did not measure band width, the outermost bands in individuals older than about two decades were narrower than the innermost visible bands. This is consistent with ossicle growth (Gage, 1990a) and overall body growth slowing at older ages, as evident in growth curves (Hirst and Forster, 2013). A consequence of the narrower width of the outer bands is that they are more difficult to unequivocally distinguish from each other, probably

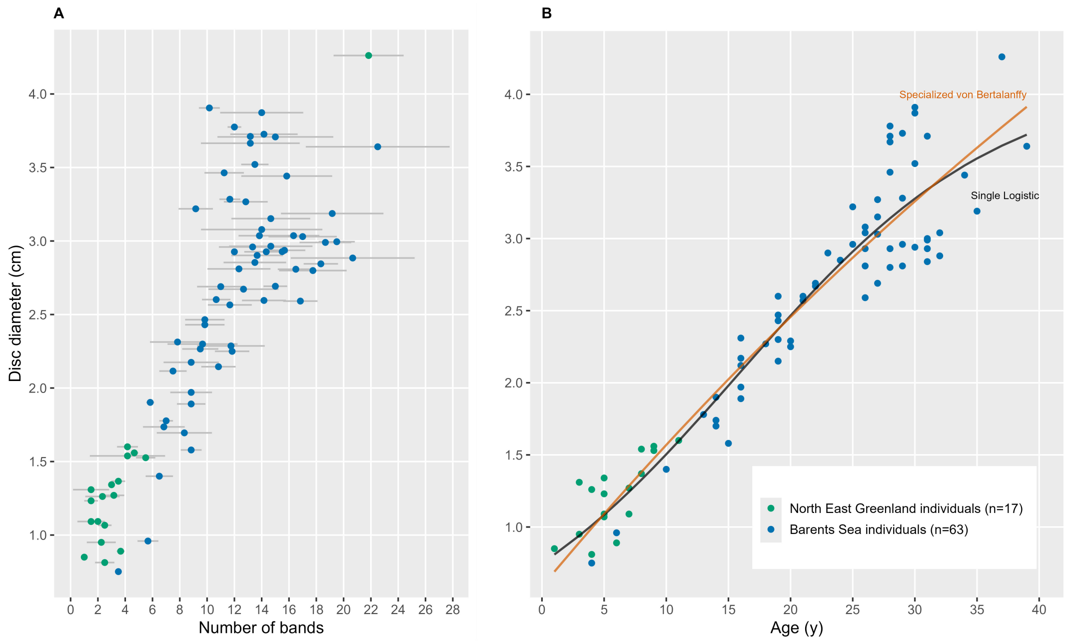

FIGURE 5
Age and growth in *Ophiopleura borealis*. **(A)** Band count (means of typically 3 ossicles ± standard deviation) across the size range of *Ophiopleura borealis* sampled, and **(B)** fitted specialized van Bertalanffy and single logistic growth curves to corrected size-at-age data. Parameter estimates for the models are in Table 1.

partly explaining the larger variation in older individuals of similar size. Some variability in the data set may also be due to somewhat different conditions at the different sampling sites.

Validating the periodicity of these bands would have been beneficial, for example, by immersing them in a stain that binds to the growing carbonate edge and then recapturing or culturing for ideally a year after marking. Some studies on other echinoderms found growth band formation not to be annual in their study species (Russell and Meredith, 2000; Hill et al., 2004; Narvaez et al., 2016). In high-latitude echinoderm species, however, validation procedures have been successful, likely because substantial to strong seasonality in environmental factors and/or food supply cause slowing of growth during unproductive times. These validations included brittle star species (Gorzula, 1977; Dahm, 1993), sea urchins (Gage, 1992; Brey et al., 1995), a sea cucumber (Sun et al., 2019), bivalves (Sejr et al., 2002a, 2002; Kilada et al., 2007) and fishes (Black et al., 2005; Kimura et al., 2007). We, therefore, have confidence in the assumption that the analyzed bands represent annual periodicity in the studied *O. borealis*.

4.2 Longevity

A maximum age of 39 years was inferred for *O. borealis*, with over half of the analyzed sample size having age estimates of ≥20 years after correction for hidden bands. As expected, age estimates generally increased with increasing body size, though there was higher variability in age-at-size and size-at-age for individuals >2.5 cm in DD and older than 25 years. Longevity estimates clearly vary among brittle star species (Table 2), although comparability is limited by differences in age estimation approaches (Gorzula, 1977; Medeiros-Bergen and Ebert, 1995). Studies differ in the skeletal parts analyzed, growth functions used, and whether age correction was applied. Regardless, a coarse comparison (Table 2) suggests a certain level of relatedness to the climatic zones of geographic distribution, generally confirming our hypothesis.

The estimated maximum age of *O. borealis* (39 years) exceeds that of all other Arctic brittle stars: *Ophiacanta bidentata* (15 years) (Stratanenko, 2021), *Stegophiura nodosa* (10 years) (Stratanenko and Denisenko, 2020), *Ophiocten sericeum* (20 years) (Ravelo et al., 2017),

TABLE 1 Model output from specialized von Bertalanffy and Single Logistic growth models applied to size-at-corrected age data of *Ophiopleura borealis*.

Parameter	*k*	t_o	*t**	S_∞	R^2	RSS	AICc
Specialized von Bertalanffy	0.01 (0.009)	-5.54 (2.06)		10.80 (7.30)	0.90	6.41	33.68
Single Logistic	0.09 (0.011)		15.89 (1.84)	4.14 (0.30)	0.90	6.09	29.53
Starting values	0.0858	-8.15	14	4.26			

k is the growth constant, S_∞ the asymptotic size, *t** the inflection point, and t_0 the age in which size is 0. Values in parentheses are standard errors. AICc, RSS and R^2 are also provided for each function. Starting values used to initiate the models with are given in the last row.

TABLE 2 Summary of maximum age estimates for brittle star species in different climatic zones including the growth constant with growth models noted were applied.

Region	Species	Age (yr)	Growth constant k_{model}	φ′	Source
Barents Sea and NE Greenland	*Ophiopleura borealis*	39	$0.01_{Specialized\ vB}$ $0.09_{Single\ Logistic}$	2.07	This study
Chukchi Sea	*Ophiura sarsii*	27	$0.077_{Gompertz}$ $0.030_{Specialized\ vB}$	1.84	(Ravelo et al., 2017)
Beaufort Sea	*Ophiocten sericeum*	20	$0.085_{Gompertz}$ $0.065_{Specialized\ vB}$	1.41	(Ravelo et al., 2017)
Vilkitsky Strait, Severnaya Zemlya	*Ophiacantha bidentata*	10-15	0.03_{vB}	4.99	(Stratanenko, 2021)
Pechora Sea	*Stegophiura nodosa*	9-10	0.09_{vB}	4.46	(Stratanenko and Denisenko, 2020)
Weddell Sea	*Ophionotus victoriae*	22	$0.12_{Richard}$ $0.25_{Richard}$	NA	(Dahm, 1996)
Weddell Sea	*Ophioplinthus gelida* (*Ophiurolepis gelida* in article)	33	0.041_{vB}	0.34	(Dahm, 1996)
Weddell Sea	*Ophioplinthus brevirima* (*Ophiurolepis brevirima* in article)	25	0.03_{vB}	-0.20	(Dahm, 1996)
Weddell Sea	*Ophioplocus incipiens (Ophioceres incipiens* in article)	19	0.007_{vB}	-0.55	(Dahm, 1996)
Weddell Sea	*Astrotoma agassizii*	91	$0.012_{\ vB}$	-0.23	(Dahm, 1996)
Chilean Sea	*Stegophiura* sp.	15	0.078_{vB} 0.095_{vB} (near cold seep)	-0.64 -0.58	(Quiroga and Sellanes, 2009)
Magellan Area, Beagle Channel	*Ophiuroglypha lymani*	20	$0.17_{Richard}$	NA	(Dahm, 1999)
Firth of Lorne, SE Scotland	*Ophiothrix fragilis*	9	0.179_{vB}	1.68	(Gage, 1990a)
West Coast of Ireland	*Amphiura filiformis*	≥20	NA	NA	(O'Connor et al., 1983)
West Coast of Ireland	*Amphiura chiajei*	≥10	NA	NA	(Munday and Keegan, 1992)
German Bight	*Ophiura ophiura*	9	0.084_{vB}	1.81	(Dahm, 1993)
German Bight	*Ophiura albida*	9	0.229_{vB}	1.37	(Dahm, 1993)
Funka Bay, SE of Hokkaido	*Ophiura sarsii (Ophiura sarsii sarsii* in article)	17	$0.23_{Gompertz}$ 0.13_{vB} $0.32_{Logistic}$ $0.067_{Richard}$	1.74	(Orino et al., 2019)
NW Scotland, SW Ireland	*Ophiocten hastatum*	10	$0.20_{Gompertz}$ $0.63_{Richard}$	NA	(Gage et al., 2004)
Rockall Trough, NW of Scotland	*Ophiocten gracilis*	7	$0.26_{Gompertz}$ 0.06_{vB}	1.44	(Gage, 2003)
Rockall Trough, NW of Scotland	*Ophiura ljungmani*	10	$0.51_{Gompertz}$ 0.27_{vB}	1.51	(Gage, 1990b)
Rockall Trough, NW of Scotland	*Ophiomusa lymani (Ophiomusium lymani* in article)	20	$0.56_{Gompertz}$ 0.36_{vB}	2.61	(Gage, 1990b)
SW Coast of New Zealand	*Astrobrachion constrictum*	8	NA	NA	(Stewart and Mladenov, 1997)
Firth of Clyde, Scotland	*Ophiocomina nigra*	12-14	NA	NA	(Gorzula, 1977)
SE Coast of Brazil	*Ophionereis reticulata*	6	$0.42_{vB\ seasonally\ oscillating}$	1.74	(Yokoyama and Amaral, 2011)

(Continued)

TABLE 2 Continued

Region	Species	Age (yr)	Growth constant k_{model}	φ′	Source
False Point, San Diego Coast	*Ophionereis annulata*	>9-11	$0.075_{Brody\text{-}Bertalanffy}$	1.48	(Medeiros-Bergen and Ebert, 1995)
False Point, San Diego Coast	*Ophioplocus esmarki*	>9-11	$0.069_{Brody\text{-}Bertalanffy}$	1.42	(Medeiros-Bergen and Ebert, 1995)

The sequence is from high to low latitudes. Growth performance (φ′) for all species was calculated in the present study. vB = von Bertalanffy. Age estimates are maximum age unless noted otherwise.

and *Ophiura sarsii* (27 years) (Ravelo et al., 2017). This may be related to the much larger body size of *O. borealis* compared to these other species. Moreover, the maximum age estimate for *O. borealis* is almost twice that reported for brittle stars from temperate regions, such as *Amphiura filiformis, Ophiomusa lymani* (referred to as *Ophiomusium lymani* in Gage, 1990) and *Ophiuroglypha lymani* which have estimated life spans of up to 20 years and are found off the west coast of Scotland and Ireland, and in the Magellan area of southern Chile, respectively (O'Connor et al., 1983; Gage, 1990a; Dahm, 1999). Estimates for sub-tropical *Ophionereis annulata* and *Ophioplocus esmarki* were nine to 11 years to reach 50% of the final body size, yet maximum age was not reported (Medeiros-Bergen and Ebert, 1995). Only brittle star estimates from the Antarctic exceed the maximum age of *O. borealis* (Dahm, 1996). Reported maximum ages in four brittle star species from the Antarctic Weddell Sea are 19, 22, 25, 33 and 91 years in *Ophioplocus incipiens* (referred to as *Ophioceres incipiens* in the article), *Ophionotus victoriae, Ophioplinthus brevirima* (referred to as *Ophiurolepis brevirima* in the article), *Ophioplinthus gelida* (referred to as *Ophiurolepis gelida* in the article) and *Astrotoma agassizii*, respectively (Dahm, 1996). Regarding the absence of age estimates in brittle stars from the tropics, the lack of seasonality in the region makes it unlikely that the brittle stars would show any pronounced growth marks. However, sampling in tropical regions would be needed to confirm this.

4.3 Growth

All referenced studies on Arctic and Antarctic brittle star species presented estimates for growth constants *k* lower than 0.1 (Table 2 and references therein), albeit estimated using different growth functions. As hypothesized, higher growth constant estimates >0.1-0.6 were more common in brittle stars from temperate regions, for example estimates for *Ophiura albida, O. sarsii* and *Ophiocten hastatum* (references in Table 2). Yet the relationship of *k* with latitude was not significant given some estimates of *k* in brittle stars from both temperate and subtropical regions were similar to those estimated for polar species (Figure 6), suggesting other factors than mere latitude also affect growth rates. Some variability in estimates of *k* was introduced by the type of

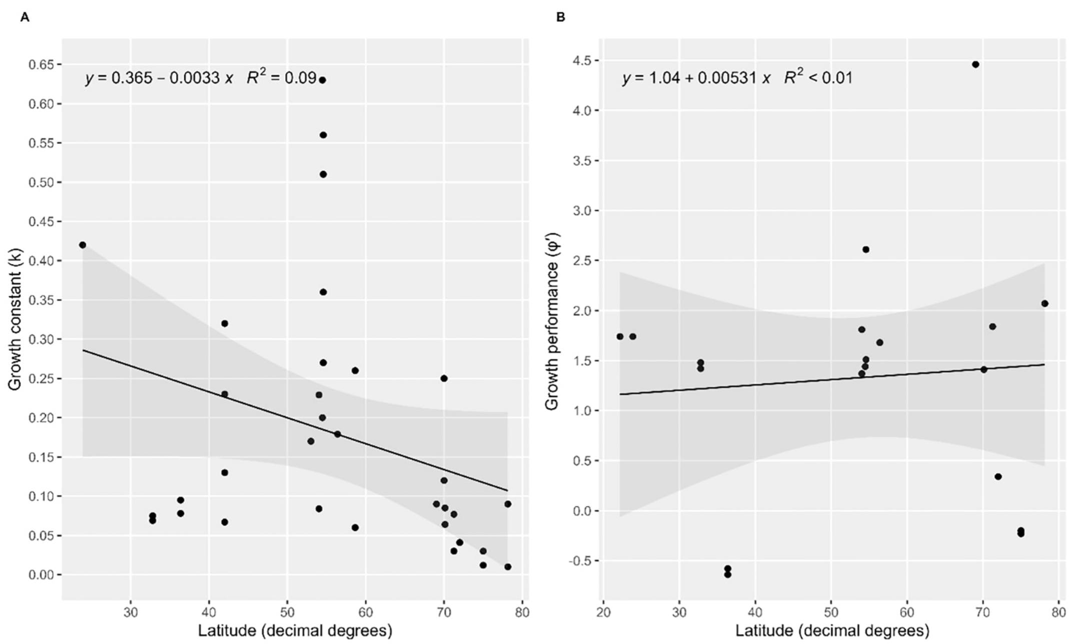

FIGURE 6
Relationships of growth metrics with latitude. **(A)** growth constant *k* versus latitude (p=0.195) and **(B)** growth performance plotted against latitude (p=0.744). Regression lines, equations with R^2-values and 95% confidence intervals (gray shade) are shown.

model used, with *k* estimates varying for the same species when different models were used with similarly good fit, as was also the case in our study. Rather than with latitude, growth rate *k* showed a positive relationship with temperature across echinoderms from various regions (Peck, 2018). Water temperature only to some degree matches latitude, since water temperature in deep water of subtropical regions, for example, is almost as low as in high latitudes, and food availability can be similarly sparse (Maier et al., 2023), both decreasing scope for growth. In contrast, a coastal subtropical species tends to experience higher temperatures and greater food availability (Hoegh-Guldberg and Pearse, 1995) supporting generally higher growth rates, yet the estimated growth constants for two shallower-water species from California (Table 2) were still low (Medeiros-Bergen and Ebert, 1995).

As differences in body sizes add variability to the comparison, growth performance (φ′) was calculated which takes body size into consideration. Using this metric, φ′ of *O. borealis* (2.07) was generally comparable to growth performances calculated for Arctic, temperate and subtropical brittle stars (mostly 1.6-2, Table 2, Figure 6). φ′ of *O. borealis* was in fact very similar to that estimated for *O. sarsii* (1.84) and *O. sericeum* (1.41; Ravelo et al., 2017), but half that estimated for the other two Arctic species *O. bidentata* (4.99) and *S. nodosa* (4.46) (Stratanenko, 2021; Stratanenko and Denisenko, 2020). Values for *Stegophiura* sp. (Quiroga and Sellanes, 2009) in the temperate zone and for all Antarctic species (Dahm, 1996) are only comparable to each other, and are somewhat lower in the polar than temperate region yet are not comparable to the remaining values as the authors used ossicle radius when applying the von Bertalanffy function.

The combination of individuals from two distinct populations in our study may have slightly affected the shape of the lower part of the growth curve. The NE Greenland shelf is overall less productive and may get even colder than the northern Barents Sea (Andrews et al., 2019), which might result in a slightly lower growth rate for the younger specimens in NE Greenland than the northern Barents Sea. While we cannot quantify the effect precisely, a comparison of growth rates in the Arctic sea urchin *Strongylocentrotus* spp. from the Barents Sea (Bluhm et al., 1998) and NE Greenland (Blicher et al., 2007) revealed similar maximum life span estimates of 42 and 45 years, respectively but a somewhat declining growth performance along the NE Greenland coast with increasing open water days (Blicher et al., 2007). Regardless, the overall low growth rate of *O. borealis* suggests that it might take many years for a population to reestablish itself after a natural or human-induced mortality event.

Several life stages of *O. borealis* have recently been studied, and together these studies begin to characterize the species' life cycle. Metabarcoding identified larvae of *O. borealis* in the upper water column in the Barents Sea in November (Descôteaux et al., 2021). Given that larvae in cold water may spend as much as a few months in the water column (Shanks, 2009), these larvae were either spawned in the autumn or perhaps as early as summer. The smallest post-larvae found at the seafloor – quite different in shape from the adults – range in size from 0.6-0.8 mm in DD (Iceland, though the time of year was not specified (Stöhr, 2005)), a size missed by our trawl gear. Subsequent growth appeared to be relatively steady over more than a decade, as the growth curve shows a near-linear increase in size with age, and a rather negligibly decrease in growth rate after the inflection point, which occurred around 16 years as estimated by the Single Logistic growth model. This rather near-linear growth was also observed in the deep-sea brittle stars *Ophiura ljungmani* (Gage and Tyler, 1982) and *Ophiocten hastatum* (Gage et al., 2004). The age at maturity is not known for *O. borealis*, but it was estimated at ca. 4 years for the temperate species *Amphiura filiformis* (Sköld et al., 2001), and one may suspect it occurs even later for *O. borealis*, given that age at maturity tends to be delayed in high-latitude species (Alvarez-Noriega et al., 2023). Typically, somatic growth in organisms slows after an organism reaches sexual maturity, because resources are then needed for gonad maturation (Lester et al., 2004). The inflection point in the Single Logistic growth curve of *O. borealis* may suggest a shift in resource allocation, perhaps related to age at maturation. Whether reproduction occurs annually thereafter is unclear, but a number of reproductive events per lifetime seem plausible, given our sample suggests that adult *O. borealis* tend to live for at least 2-3, if not 4, decades.

5 Conclusion

This study has demonstrated that growth bands are indeed present in the Arctic brittle star *Ophiopleura borealis* and has provided the first age estimates for this large species. The maximum estimated age, 39 years, exceeds all maximum ages reported for brittle stars from lower latitudes. The estimated growth constants for *O. borealis* were low and similar to those estimated for other polar brittle stars, although a few temperate and subtropical species exhibited even lower growth constant estimates; growth performance was broadly comparable to other brittle stars across latitudes. The combination of slow growth and long lifespan may render *O. borealis* less resilient to disturbances compared to faster-growing species. We recommend conducting longevity studies on additional high-latitude invertebrate species to be able to evaluate their sensitivity to increasing exposure to a suite of stressors, with validation of growth band periodicity included.

Data availability statement

The original contributions presented in the study are included in the article/Supplementary Material. Further inquiries can be directed to the corresponding author.

Ethics statement

The manuscript presents research on animals that do not require ethical approval for their study.

Author contributions

HD: Conceptualization, Formal Analysis, Investigation, Methodology, Writing – original draft, Writing – review & editing. AA: Conceptualization, Methodology, Supervision, Validation, Writing – review & editing. BB: Conceptualization, Funding acquisition, Investigation, Methodology, Project administration, Supervision, Writing – review & editing.

Funding

The author(s) declare that financial support was received for the research, and/or publication of this article. Funding was provided by The Research Council of Norway through the Nansen Legacy project (#276730), and through an Erasmus stipend to HD.

Acknowledgments

We thank the Arctic PRIZE, Nansen Legacy (Research Council of Norway, grant number 276730), and TUNU field teams for sample collection. We thank Joel Vikberg Wernström and Vanessa Pitusi, UiT - The Arctic University of Norway, for their support in the laboratory, and UArctic for support through the thematic network on Arctic Marine Biodiversity.

Conflict of interest

The authors declare that the research was conducted in the absence of any commercial or financial relationships that could be construed as a potential conflict of interest.

Generative AI statement

The author(s) declare that no Generative AI was used in the creation of this manuscript.

Publisher's note

Supplementary material

The Supplementary Material for this article can be found online at: https://www.frontiersin.org/articles/10.3389/fmars.2025.1555911/full#supplementary-material

References

Al-Habahbeh, A. K., Kortsch, S., Bluhm, B. A., Beuchel, F., Gulliksen, B., Ballantine, C., et al. (2020). Arctic coastal benthos long-term responses to perturbations under climate warming. *Philos. Trans. A Math Phys. Eng. Sci.* 378, 20190355. doi: 10.1098/rsta.2019.0355

Alvarez-Noriega, M., White, C. R., Kozlowski, J., Day, T., and Marshall, D. J. (2023). Life history optimisation drives latitudinal gradients and responses to global change in marine fishes. *PLoS Biol.* 21, e3002114. doi: 10.1371/journal.pbio.3002114

Ambrose, W. G., Clough, L. M., Tilney, P. R., and Beer, L. (2001). Role of echinoderms in benthic remineralization in the Chukchi Sea. *Mar. Biol.* 139, 937–949. doi: 10.1007/s002270100652

Andrews, A. J., Christiansen, J. S., Bhat, S., Lynghammar, A., Westgaard, J. I., Pampoulie, C., et al. (2019). Boreal marine fauna from the Barents Sea disperse to Arctic Northeast Greenland. *Sci. Rep.* 9, 5799. doi: 10.1038/s41598-019-42097-x

Aphalo, P. J. (2016). *ggpmisc: Miscellaneous Extensions to 'ggplot2'*. doi: 10.32614/CRAN.package.ggpmisc

Aven, T., and Renn, O. (2012). On the risk management and risk governance of petroleum operations in the Barents Sea area. *Risk Anal.* 32, 1561–1575. doi: 10.1111/j.1539-6924.2011.01777.x

Beuchel, F., and Gulliksen, B. (2008). Temporal patterns of benthic community development in an Arctic fjord (Kongsfjorden, Svalbard): results of a 24-year manipulation study. *Polar Biol.* 31, 913–924. doi: 10.1007/s00300-008-0429-9

Black, B. A., Boehlert, G. W., and Yoklavich, M. M. (2005). Using tree-ring crossdating techniques to validate annual growth increments in long-lived fishes. *Can. J. Fish Aquat Sci.* 62, 2277–2284. doi: 10.1139/f05-142

Blicher, M. E., Rysgaard, S., and Sejr, M. K. (2007). Growth and production of sea urchin *Strongylocentrotus droebachiensis* in a high-Arctic fjord, and growth along a climatic gradient (64 to 77°N). *Mar. Ecol. Prog. Ser.* 341, 89–102. doi: 10.3354/meps341089

Blicher, M. E., and Sejr, M. K. (2011). Abundance, oxygen consumption and carbon demand of brittle stars in Young Sound and the NE Greenland shelf. *Mar. Ecol. Prog. Ser.* 422, 139–144. doi: 10.3354/meps08915

Bluhm, B. A., Iken, K., Hardy, S. M., Sirenko, B. I., and Holladay, B. A. (2009). Community structure of epibenthic megafauna in the Chukchi Sea. *Aquat Biol.* 7, 269–293. doi: 10.3354/ab00198

Bluhm, B. A., Piepenburg, D., and Von Juterzenka, K. (1998). Distribution, standing stock, growth, mortality and production of *Strongylocentrotus pallidus* (Echinodermata: Echinoidea) in the northern Barents Sea. *Polar Biol.* 20, 325–334. doi: 10.1007/s003000050310

Bonfim, M., Lopez, D. P., Repetto, M. F., and Freestone, A. L. (2024). Speed and degree of functional and compositional recovery varies with latitude and community age. *Ecology* 105, e4259. doi: 10.1002/ecy.4259

Brey, T. (2001). *Population dynamics in benthic invertebrates. A virtual handbook. Version 01.2.* Available online at: http://www.thomas-brey.de/science/virtualhandbook.

Brey, T., Pearse, J., Basch, L., Mcclintock, J., and Slattery, M. (1995). Growth and production of *Sterechinus neumayeri* (Echinoidea: Echinodermata) in McMurdo sound, Antarctica. *Mar. Biol.* 124, 279–292. doi: 10.1007/Bf00347132

Broach, K. H., Miller, M. F., and Bowser, S. S. (2016). Bioturbation by the common Antarctic scallop (*Adamussium colbecki*) and ophiuroid (*Ophionotus victoriae*) under multi-year sea ice: Ecologic and stratigraphic implications. *Palaios* 31, 280–290. doi: 10.2110/palo.2015.069

Broom, D. M. (2009). Aggregation behaviour of the brittle-star *Ophiothrix fragilis*. *J. Mar. Biol. Assoc. U K* 55, 191–197. doi: 10.1017/s0025315400015836

Burukovsky, R. N., Syomin, V. L., Zalota, A. K., Simakov, M. I., and Spiridonov, V. A. (2022). Food spectra of snow crabs (*Chionoecetes opilio* (O. Fabricius 1788) (Decapoda, Oregoniidae), non-indigenous species of the Kara Sea. *Oceanology* 61, 964–975. doi: 10.1134/s0001437021060205

Calero, B., Ramos, A., and Ramil, F. (2018). An uncommon or just an ecologically demanding species? Finding of aggregations of the brittle-star *Ophiothrix maculata* on the Northwest African slope. *Deep-Sea Res. Pt I* 131, 87–92. doi: 10.1016/j.dsr.2017.11.008

Calvet, N., Bluhm, B. A., Yoccoz, N. G., and Altenburger, A. (2024). Shifting invertebrate distributions in the Barents Sea since pre-1900. *Front. Mar. Sci.* 11. doi: 10.3389/fmars.2024.1421475

Christiansen, J. S. (2012). "The TUNU-programme: euro-arctic marine fishes—Diversity and adaptation," in *Adaptation and Evolution in Marine Environments*, vol. 1. Eds. G. Di Prisco and C. Verde (Springer Berlin Heidelberg, Berlin, Heidelberg), 35–50.

Dahm, C. (1993). Growth, production and ecological significance of *Ophiura albida* and *O. ophiura* (Echinodermata, Ophiuroidea) in the German Bight. *Mar. Biol.* 116, 431–437. doi: 10.1007/Bf00350060

Dahm, C. (1996). *Ökologie und Populationsdynamik antarktischer Ophiuroiden (Echinodermata) = Ecology and population dynamics of Antarctic ophiuroids (Echinodermata)* (Bremerhaven: Alfred Wegener Institute for Polar and Marine Research). doi: 10.2312/BzP_0194_1996

Dahm, C. (1999). Ophiuroids (Echinodermata) of southern Chile and the Antarctic: taxonomy, biomass, diet and growth of dominant species. *Sci. Mar.* 63, 427–432. doi: 10.3989/scimar.1999.63s1427

Dahm, C., and Brey, T. (1998). Determination of growth and age of slow growing brittle stars (Echinodermata: Ophiuroidea) from natural growth bands. *J. Mar. Biol. Assoc. U K* 78, 941–951. doi: 10.1017/S0025315400044891

Danielssen, D. C., and Koren, J. (1877). Fra den norske Nordhavsexpedition: Echinodermer. *Nyt magazin for naturvidenskaberne.* 23 (3), 45–83.

Dantzer, B., and Fletcher, Q. E. (2015). Telomeres shorten more slowly in slow-aging wild animals than in fast-aging ones. *Exp. Gerontol.* 71, 38–47. doi: 10.1016/j.exger.2015.08.012

Davoult, D., Harlay, J., and Gentil, F. (2009). Contribution of a dense population of the Brittle Star *Acrocnida brachiata* (Montagu) to the biogeochemical fluxes of CO_2 in a temperate coastal ecosystem. *Estuar. Coast.* 32, 1103–1110. doi: 10.1007/s12237-009-9216-2

Davoult, D., and Migné, A. (2001). "Respiration and excretion of a dense *Ophiothrix fragilis* population in the Bay of Seine (English Channel, France)," in *Echinoderm 2000*. Ed. B. M. Balkema, 243–248.

Descôteaux, R., Ershova, E., Wangensteen, O. S., Præbel, K., Renaud, P. E., Cottier, F., et al. (2021). Meroplankton diversity, seasonality and life-history traits across the Barents Sea Polar Front revealed by high-throughput DNA barcoding. *Front. Mar. Sci.* 8. doi: 10.3389/fmars.2021.677732

Elzhov, T. V., Mullen, K. M., Spiess, A.-N., and Bolker, B. (2022). *minpack.lm: R Interface to the Levenberg-Marquardt nonlinear least-squares algorithm found in MINPACK, Plus Support for Bounds*. doi: 10.32614/CRAN.package.minpack.lm

Fujita, T., and Ohta, S. (1989). Spatial structure within a dense bed of the brittle star *Ophiura sarsi* (Ophiuroidea: Echinodermata) in the bathyal zone off Otsuchi, Northeastern Japan. *J. Oceanogr* 45, 289–300. doi: 10.1007/bf02123483

Fujita, T., and Ohta, S. (1990). Size structure of dense populations of the brittle star *Ophiura sarsii* (Ophiuroidea, Echinodermata) in the bathyal zone around Japan. *Mar. Ecol. Prog. Ser.* 64, 113–122. doi: 10.3354/meps064113

Gage, J. D. (1990a). Skeletal growth bands in brittle stars - microstructure and significance as age markers. *J. Mar. Biol. Assoc. U K* 70, 209–224. doi: 10.1017/S0025315400034329

Gage, J. D. (1990b). Skeletal growth markers in the deep-sea brittle stars *Ophiura ljungmani* and *Ophiomusium lymani*. *Mar. Biol.* 104, 427–435. doi: 10.1007/bf01314346

Gage, J. D. (1992). Natural growth bands and growth variability in the sea-urchin *Echinus esculentus* - Results from tetracycline tagging. *Mar. Biol.* 114, 607–616. doi: 10.1007/Bf00357257

Gage, J. D. (2003). Growth and production of *Ophiocten gracilis* (Ophiuroidea: Echinodermata) on the Scottish continental slope. *Mar. Biol.* 143, 85–97. doi: 10.1007/s00227-003-1050-7

Gage, J. D., Anderson, R. M., Tyler, P. A., Chapman, R., and Dolan, E. (2004). Growth, reproduction and possible recruitment variability in the abyssal brittle star *Ophiocten hastatum* (Ophiuroidea: Echinodermata) in the NE Atlantic. *Deep-Sea Res. Pt I* 51, 849–864. doi: 10.1016/S0967-0637(04)00032-9

Gage, J. D., and Tyler, P. A. (1982). Depth-related gradients in size structure and the bathymetric zonation of deep-sea brittle stars. *Mar. Biol.* 71, 299–308. doi: 10.1007/Bf00397046

Galkin, S. V., Kucheruk, N. V., Minin, K. V., Rayskiy, A. K., and Goroslavskaya, E. I. (2010a). Macrobenthos of the Ob River estuarine zone and of the adjacent regions of the Kara Sea. *Oceanology* 50, 793–797. doi: 10.1134/S0001437010050152

Galkin, S. V., Savilova, T. A., Moskalev, L. I., and Kucheruk, N. V. (2010b). Macrobenthos of the Novaya Zemlya trough. *Oceanology* 50, 933–944. doi: 10.1134/S0001437010060135

Galkin, S. V., Vedenin, A. A., Minin, K. V., Rogacheva, A. V., Molodtsova, T. N., Rajskiy, A. K., et al. (2015). Macrobenthos of the southern part of St. Anna Trough and the adjacent Kara Sea shelf. *Oceanology* 55, 614–622. doi: 10.1134/S0001437015040098

Gallagher, M. L., Ambrose, W. G., and Renaud, P. E. (1998). Comparative studies in biochemical composition of benthic invertebrates (bivalves, ophiuroids) from the Northeast Water (NEW) Polynya. *Polar Biol.* 19, 167–171. doi: 10.1007/s003000050230

Gorzula, S. (1977). A study of growth in the brittle-star *Ophiocomina nigra*. *Western Nat.* 6, 13–33.

Hill, S. K., Aragona, J. B., and Lawrence, J. M. (2004). Growth bands in test plates of the sea urchins *Arbacia punctulata* and *Lytechinus variegatus* (Echinodermata) on the Central Florida Gulf Coast Shelf. *Gulf Mex Sci.* 22, 96–100. doi: 10.18785/goms.2201.09

Hinz, H., Kröncke, I., and Ehrich, S. (2005). The feeding strategy of dab *Limanda limanda* in the southern North Sea: linking stomach contents to prey availability in the environment. *J. Fish Biol.* 67, 125–145. doi: 10.1111/j.0022-1112.2005.00918.x

Hirst, A. G., and Forster, J. (2013). When growth models are not universal: evidence from marine invertebrates. *Proc. Biol. Sci.* 280, 20131546. doi: 10.1098/rspb.2013.1546

Hoegh-Guldberg, O. V. E., and Pearse, J. S. (1995). Temperature, food availability, and the development of marine invertebrate larvae. *Am. Zool* 35, 415–425. doi: 10.1093/icb/35.4.415

Hopkins, J. (2018). *RRS James Clark Ross JR16006: 30 June-8 Aug 2017, the Changing Arctic Ocean Cruise JR16006: cruise report.*

Hüssy, K., Andersen, N. G., and Pedersen, E. M. (2016). The influence of feeding behaviour on growth of Atlantic cod (*Gadus morhua*, Linnaeus 1758) in the North Sea. *J. Appl. Ichthyol* 32, 928–937. doi: 10.1111/jai.13160

Ingvaldsen, R., Bluhm, B., Aberle-Malzahn, N., Amundsen, R., Van Ardelan, M., Bagøien, E., et al. (2020). Joint cruise 1-2 2018. *Nansen Legacy Rep. Series.* doi: 10.7557/nlrs.5628

Jakobsen, T., and Ozhigin, V. K. (2011). *The Barents Sea. Ecosystem, Resources, Management. Half a century of Russian - Norwegian cooperation* (Trondheim, Norway: Tapir Academic Press).

Jørgensen, L. L., Ljubin, P., Skjoldal, H. R., Ingvaldsen, R. B., Anisimova, N., and Manushin, I. (2015). Distribution of benthic megafauna in the Barents Sea: baseline for an ecosystem approach to management. *Ices J. Mar. Sci.* 72, 595–613. doi: 10.1093/icesjms/fsu106

Jørgensen, L. L., Planque, B., Thangstad, T. H., and Certain, G. (2016). Vulnerability of megabenthic species to trawling in the Barents Sea. *Ices J. Mar. Sci.* 73, i84–i97. doi: 10.1093/icesjms/fsv107

Kassambara, A. (2023). *ggpubr: 'ggplot2' Based Publication Ready Plots*. doi: 10.32614/CRAN.package.ggpubr

Kilada, R. W., Campana, S. E., and Roddick, D. (2007). Validated age, growth, and mortality estimates of the ocean quahog (*Arctica islandica*) in the western Atlantic. *Ices J. Mar. Sci.* 64, 31–38. doi: 10.1093/icesjms/fsl001

Kimura, D., Anderl, D., and Goetz, B. (2007). Seasonal marginal growth on otoliths of seven Alaska groundfish species support the existence of annual patterns. *Alsk Fish Res. Bull.* 12, 243–251.

Kortsch, S., Primicerio, R., Beuchel, F., Renaud, P. E., Rodrigues, J., Lonne, O. J., et al. (2012). Climate-driven regime shifts in Arctic marine benthos. *Proc. Natl. Acad. Sci. U.S.A.* 109, 14052–14057. doi: 10.1073/pnas.1207509109

Lebrato, M., Iglesias-Rodriguez, D., Feely, R. A., Greeley, D., Jones, D. O. B., Suarez-Bosche, N., et al. (2010). Global contribution of echinoderms to the marine carbon cycle: $CaCO_3$ budget and benthic compartments. *Ecol. Monogr.* 80, 441–467. doi: 10.1890/09-0553.1

Lester, N. P., Shuter, B. J., and Abrams, P. A. (2004). Interpreting the von Bertalanffy model of somatic growth in fishes: the cost of reproduction. *Proc. Biol. Sci.* 271, 1625–1631. doi: 10.1098/rspb.2004.2778

Levin, L. A., Sibuet, M., Gooday, A. J., Smith, C. R., and Vanreusel, A. (2010). The roles of habitat heterogeneity in generating and maintaining biodiversity on continental margins: an introduction. *Mar. Ecol-Evol Persp.* 31, 1–5. doi: 10.1111/j.1439-0485.2009.00358.x

Maier, S. R., Brooke, S., De Clippele, L. H., De Froe, E., van der Kaaden, A. S., Kutti, T., et al. (2023). On the paradox of thriving cold-water coral reefs in the food-limited deep sea. *Biol. Rev. Camb Philos. Soc.* 98, 1768–1795. doi: 10.1111/brv.12976

Mazerolle, M. J. (2023). *AICcmodavg: Model selection and multimodel inference based on (Q)AIC(c). R package version 2.3.3.* doi: 10.32614/CRAN.package.AICcmodavg

Medeiros-Bergen, D. E., and Ebert, T. A. (1995). Growth, fecundity and mortality rates of two intertidal brittlestars (Echinodermata: Ophiuroidea) with contrasting modes of development. *J. Exp. Mar. Biol. Ecol.* 189, 47–64. doi: 10.1016/0022-0981(95)00010-o

Moore, J. C., and de Ruiter, P. C. (2012). *Energetic Food Webs: An analysis of real and model ecosystems* (Oxford: Oxford University Press). doi: 10.1093/acprof:oso/9780198566182.001.0001

Munday, B. W., and Keegan, B. F. (1992). Population-dynamics of *Amphiura chiajei* (Echinodermata, Ophiuroidea) in Killary Harbor, on the west-coast of Ireland. *Mar. Biol.* 114, 595–605. doi: 10.1007/Bf00357256

Murat, A., Méar, Y., Poizot, E., Dauvin, J. C., and Beryouni, K. (2016). Silting up and development of anoxic conditions enhanced by high abundance of the geoengineer species. *Cont Shelf Res.* 118, 11–22. doi: 10.1016/j.csr.2016.01.003

Narvaez, C. A., Johnson, L. E., and Sainte-Marie, B. (2016). Growth bands are an unreliable indicator of sea urchin age: Evidence from the laboratory and the literature. *Limnol. Oceanogr. Methods* 14, 527–541. doi: 10.1002/lom3.10110

Neves, B. D., Edinger, E., Layne, G. D., and Wareham, V. E. (2015). Decadal longevity and slow growth rates in the deep-water sea pen *Halipteris finmarchica* (Sars 1851) (Octocorallia: Pennatulacea): implications for vulnerability and recovery from anthropogenic disturbance. *Hydrobiologia* 759, 147–170. doi: 10.1007/s10750-015-2229-x

O'Connor, B., Bowmer, T., and Grehan, A. (1983). Long-term assessment of the population dynamics of *Amphiura filiformis* (Echinodermata: Ophiuroidea) in Galway Bay (west coast of Ireland). *Mar. Biol.* 75, 279–286. doi: 10.1007/bf00406013

Orino, K., Ishigane, K., Suzuki, K., Izumiura, H., Nakaya, M., and Takatsu, T. (2019). Growth of the brittle star *Ophiura sarsii sarsii* in Funka Bay, Hokkaido, Japan. *Fisheries Sci.* 85, 705–716. doi: 10.1007/s12562-019-01323-1

Pavlova, L. V., Dvoretsky, A. G., Frolov, A. A., Zimina, O. L., Evseeva, O. Y., Dikaeva, D. R., et al. (2023). The impact of sea ice loss on benthic communities of the Makarov strait (Northeastern Barents Sea). *Animals* 13, 2320. doi: 10.3390/ani13142320

Peck, L. S. (2016). A cold limit to adaptation in the sea. *Trends Ecol. Evol.* 31, 13–26. doi: 10.1016/j.tree.2015.09.014

Peck, L. S. (2018). Antarctic marine biodiversity: adaptations, environments and responses to change. *Oceanography Mar. Biol. - Annu. Rev.* 65, 2–133. doi: 10.1201/9780429454455

Pedersen, T., Nilsen, M., Nilssen, E. M., Berg, E., and Reigstad, M. (2008). Trophic model of a lightly exploited cod-dominated ecosystem. *Ecol. Model.* 214, 95–111. doi: 10.1016/j.ecolmodel.2007.12.012

Piepenburg, D. (2000). Arctic brittle stars (Echinodermata: Ophiuroidea). *Oceanogr Mar. Biol.* 38, 189–256.

Piepenburg, D., and Schmid, M. K. (1996). Distribution, abundance, biomass, and mineralization potential of the epibenthic megafauna of the Northeast Greenland shelf. *Mar. Biol.* 125, 321–332. doi: 10.1007/Bf00346313

Piepenburg, D., and Schmid, M. K. (1997). A photographic survey of the epibenthic megafauna of the Arctic Laptev Sea shelf: Distribution, abundance, and estimates of biomass and organic carbon demand. *Mar. Ecol. Prog. Ser.* 147, 63–75. doi: 10.3354/meps147063

Piepenburg, D., and Von Juterzenka, K. (1994). Abundance, biomass and spatial-distribution pattern of brittle stars (Echinodermata, Ophiuroidea) on the Kolbeinsey Ridge North of Iceland. *Polar Biol.* 14, 185–194. doi: 10.1007/Bf00240523

Piepenburg, D., Voss, J., and Gutt, J. (1997). Assemblages of sea stars (Echinodermata: Asteroidea) and brittle stars (Echinodermata: Ophiuroidea) in the Weddell Sea (Antarctica) and off Northeast Greenland (Arctic): A comparison of diversity and abundance. *Polar Biol.* 17, 305–322. doi: 10.1007/Pl00013372

Pörtner, H. O., Langenbuch, M., and Michaelidis, B. (2005). Synergistic effects of temperature extremes, hypoxia, and increases in CO_2 on marine animals: From Earth history to global change. *J. Geophys Res. Oceans* 110. doi: 10.1029/2004jc002561

Quiroga, E., and Sellanes, J. (2009). Growth and size-structure of *Stegophiura* sp. (Echinodermata: Ophiuroidea) on the continental slope off central Chile: a comparison between cold seep and non-seep sites. *J. Mar. Biol. Assoc. U K* 89, 421–428. doi: 10.1017/S0025315408002786

Ravelo, A. M., Konar, B., Bluhm, B., and Iken, K. (2017). Growth and production of the brittle stars *Ophiura sarsii* and *Ophiocten sericeum* (Echinodermata: Ophiuroidea). *Cont Shelf Res.* 139, 9–20. doi: 10.1016/j.csr.2017.03.011

Ravelo, A. M., Konar, B., Trefry, J. H., and Grebmeier, J. M. (2014). Epibenthic community variability in the northeastern Chukchi Sea. *Deep-Sea Res. Pt Ii* 102, 119–131. doi: 10.1016/j.dsr2.2013.07.017

R Core Team (2023). *R: A language and environment for statistical computing. R Foundation for Statistical Computing* (Vienna, Austria).

Reigstad, M., Johnsen, G., and Sundfjord, A. (in press). *The Barents Sea system – gateway to the changing Arctic* (Fagbokforlaget, Bergen).

Russell, M. P., and Meredith, R. W. (2000). Natural growth lines in echinoid ossicles are not reliable indicators of age: a test using *Strongylocentrotus droebachiensis*. *Invertebr Biol.* 119, 410–420. doi: 10.1111/j.1744-7410.2000.tb00111.x

Salguero-Gómez, R., and Jones, O. R. (2017). "Life history trade-offs modulate the speed of senescence," in *The Evolution of Senescence in the Tree of Life*. Eds. R. P. Shefferson, O. R. Jones and R. Salguero-Gómez (Cambridge University Press, Cambridge), 403–421.

Schneider, C. A., Rasband, W. S., and Eliceiri, K. W. (2012). NIH Image to ImageJ: 25 years of image analysis. *Nat. Methods* 9, 671–675. doi: 10.1038/nmeth.2089

Sejr, M. K., Jensen, K. T., and Rysgaard, S. (2002a). Annual growth bands in the bivalve *Hiatella arctica* validated by a mark-recapture study in NE Greenland. *Polar Biol.* 25, 794–796. doi: 10.1007/s00300-002-0413-8

Sejr, M. K., Sand, M. K., Jensen, K. T., Petersen, J. K., Christensen, P. B., and Rysgaard, S. (2002b). Growth and production of *Hiatella arctica* (Bivalvia) in a high-Arctic fjord (Young Sound, Northeast Greenland). *Mar. Ecol. Prog. Ser.* 244, 163–169. doi: 10.3354/meps244163

Shanks, A. L. (2009). Pelagic larval duration and dispersal distance revisited. *Biol. Bull.* 216, 373–385. doi: 10.1086/BBLv216n3p373

Skagseth, Ø., Eldevik, T., Årthun, M., Asbjørnsen, H., Lien, V. S., and Smedsrud, L. H. (2020). Reduced efficiency of the Barents Sea cooling machine. *Nat. Climate Change* 10, 661–666. doi: 10.1038/s41558-020-0772-6

Sköld, M., Josefson, A., and Loo, L.-O. (2001). Sigmoidal growth in the brittle star *Amphiura filiformis* (Echinodermata: Ophiuroidea). *Mar. Biol.* 139, 519–526. doi: 10.1007/s002270100600

Smirnov, I. S., Piepenburg, D., Ahearn, C., and Juterzenka, K. V. (2014). Deep-sea fauna of European seas: An annotated species check-list of benthic invertebrates living deeper than 2000 m in the seas bordering Europe. Ophiuroidea. *Invertebr. Zool.* 11, 192–209. doi: 10.15298/invertzool.11.1.18

Stearns, S. C., and Koella, J. C. (1986). The evolution of phenotypic plasticity in life-history traits: predictions of reaction norms for age and size at maturity. *Evolution* 40, 893–913. doi: 10.1111/j.1558-5646.1986.tb00560.x

Stewart, B. G., and Mladenov, P. V. (1997). Population structure, growth and recruitment of the euryalinid brittle-star *Astrobrachion constrictum* (Echinodermata: Ophiuroidea) in Doubtful Sound, Fiordland, New Zealand. *Mar. Biol.* 127, 687–697. doi: 10.1007/s002270050059

Stöhr, S. (2005). Who's who among baby brittle stars (Echinodermata: Ophiuroidea): postmetamorphic development of some North Atlantic forms. *Zool J. Linn Soc.* 143, 543–576. doi: 10.1111/j.1096-3642.2005.00155.x

Stöhr, S., O'hara, T. D., and Thuy, B. (2012). Global diversity of brittle stars (Echinodermata: Ophiuroidea). *PloS One* 7, e31940. doi: 10.1371/journal.pone.0031940

Stratanenko, E. A. (2021). A comparative analysis of the growth and lifespan of *Ophiacantha bidentata* Retzius 1805 (Echinodermata, Ophiuroidea) in the high latitudes of the Russian Arctic. *Biol. Bull.* 48, 1263–1271. doi: 10.1134/S1062359021080276

Stratanenko, E. A., and Denisenko, S. G. (2020). Growth of *Stegophiura nodosa* (Echinodermata, Ophiuroidea) in the Pechora Sea. *J. Mar. Biol. Assoc. U K* 100, 1129–1133. doi: 10.1017/S0025315420001010

Sun, J., Hamel, J. F., Gianasi, B. L., and Mercier, A. (2019). Age determination in echinoderms: first evidence of annual growth rings in holothuroids. *Proc. Biol. Sci.* 286, 20190858. doi: 10.1098/rspb.2019.0858

Udalov, A. A., Vedenin, A. A., and Chava, A. I. (2018). Benthic fauna of Stepovoi Bay (Novaya Zemlya Archipelago, Kara Sea). *Oceanology* 58, 838–846. doi: 10.1134/S0001437018060140

Vopel, K., Thistle, D., and Rosenberg, R. (2003). Effect of the brittle star *Amphiura filiformis* (Amphiuridae, Echinodermata) on oxygen flux into the sediment. *Limnol Oceanogr* 48, 2034–2045. doi: 10.4319/lo.2003.48.5.2034

Wickham, H., Chang, W., Henry, L., Pedersen, T. L., Takahashi, K., Wilke, C., et al. (2007). *ggplot2: Create Elegant Data Visualisations Using the Grammar of Graphics*. doi: 10.32614/CRAN.package.ggplot2

Wickham, H., François, R., Henry, L., Müller, K., and Vaughan, D. (2014). *dplyr: A Grammar of Data Manipulation*. doi: 10.32614/CRAN.package.dplyr

Wood, H. L., Spicer, J. I., and Widdicombe, S. (2008). Ocean acidification may increase calcification rates, but at a cost. *Proc. Biol. Sci.* 275, 1767–1773. doi: 10.1098/rspb.2008.0343

Yokoyama, L. Q., and Amaral, A. C. Z. (2011). Recruitment and growth variation of *Ophionereis reticulata* (Echinodermata: Ophiuroidea). *Invertebr Reprod. Dev.* 55, 73–81. doi: 10.1080/07924259.2011.553402

Yunda-Guarin, G., Michel, L. N., Nozais, C., and Archambault, P. (2022). Interspecific differences in feeding selectivity shape isotopic niche structure of three ophiuroids in the Arctic Ocean. *Mar. Ecol. Prog. Ser.* 683, 81–95. doi: 10.3354/meps13965

Zhulay, I., Iken, K., Renaud, P. E., and Bluhm, B. A. (2019). Epifaunal communities across marine landscapes of the deep Chukchi Borderland (Pacific Arctic). *Deep-Sea Res. Pt I* 151, 103065. doi: 10.1016/j.dsr.2019.06.011